Dominant Radiative Transitions

of the

Low-lying Charmonium Excited States

Gurjav Ganbold

Bogolubov Laboratory of Theoretical Physics, JINR, Dubna

Institute of Physics and Technology, MAS, Ulaanbaatar

in collaboration with T.Gutsche (Tuebingen University),
M.A.Ivanov (BLTP JINR),
V.Lyubovitskij (Tuebingen University)

Outline

- **Motivation**

- **Low-lying charmonium ground states and orbital (L=1) excitations**
  - **Dominant (one-photon) radiative decays of states:**

• **Vector**	1^{--}	J/Ψ
• **Scalar**	0^{++}	χ_{c0}
• **Axial Vector**	1^{++}	χ_{c1}
• **Axial Vector**	1^{+-}	h_c
• **Tensor**	2^{++}	χ_{c2}

- **Approach (CCQM)**
  - **Interaction: Hadron - Interpolating quark current**
  - **Compositeness condition**
  - **Infrared confinement (cutoff)**

- **Numerical results:**
  - **Model parameters**
  - **Renormalized couplings**
  - **Decay widths**
  - **Deconfinement limit**

- **Summary and outlook**

Charmonium Radiative Decays

Charmonium states $^{2S+1}L_J$ ($L \le 1$): dominant radiative decay modes PDG-2021

State	J^{PC}	Current	Mass (MeV)	Full width (Γ)	Mode	Fraction (Γ_i / Γ)
$\eta_c(^1S_0)$	0^{-+}	$i\bar{q}\gamma_5 q$	2983.9 ± 0.5	32.0 ± 0.7 MeV	$\gamma + \gamma$	(1.58 ± 0.11) x 10^{-4}
$J/\Psi(^3S_1)$	1^{--}	$\bar{q}\gamma_\mu q$	3096.9 ± 0.0006	92.9 ± 2.8 keV	$\gamma + h_c$	(1.7 ± 0.4) x 10^{-4}
$\chi_{c0}(^3P_0)$	0^{++}	$\bar{q} I q$	3414.71 ± 0.30	10.8 ± 0.6 MeV	$\gamma + J/\Psi$	(1.40 ± 0.05) x 10^{-4}
$\chi_{c1}(^3P_1)$	1^{++}	$\bar{q}\,\gamma_\mu\,\gamma_5 q$	3510.67 ± 0.05	0.84 ± 0.04 MeV	$\gamma + J/\Psi$	(34.3 ± 1.0) x 10^{-4}
$h_c(^1P_1)$	1^{+-}	$i\bar{q}\,\overleftrightarrow{\partial}_\mu\,\gamma_5 q$	3525.38 ± 0.11	0.7 ± 0.4 MeV	$\gamma + h_c$	(51 ± 6) x 10^{-4}
$\chi_{c2}(^3P_2)$	2^{++}	$\frac{i}{2}\bar{q}\left(\gamma_\mu \overleftrightarrow{\partial}_\nu + \gamma_\nu \overleftrightarrow{\partial}_\mu\right) q$	3556.17 ± 0.07	1.97 ± 0.09 MeV	$\gamma + J/\Psi$	(19.0 ± 0.5) x 10^{-4}

- ***These charmonium states are unusual:***
  - *the c-quark mass is much larger than the confinement scale*
  - *they have low-lying excited states ($L = 1$, $J^{PC} = 0^{++}, 1^{++}, 1^{+-}, 2^{++}$).*
- ***Low-lying $c\bar{c}$ mesons***
  - *have narrow widths,*
  - *their dominant radiative transitions are one-photon decay modes.*
- ***Charmonium states below the $D\bar{D}$ threshold have been intensively searched, observed and measured fairly accurately** (LHCb, BES-III, BELLE, …).*

♦ ***Small binding energy -> an ideal testing ground to validate model assumptions:***

- **Quark potential models**
- **Lattice simulations QCD**
- **QCD sum rules**
- **Effective Lagrangian approaches**
- **Nonrelativistic effective field theories of QCD**
- **Constituent quark models**
- **Approaches based on the Bethe-Salpeter equations**
- **Light-front quark model**
- **Coulomb gauge approach**

Discrepancies still exist between the theoretical predictions and world data:

- **Nonrelativistic potential model [12] and in the Coulomb gauge approach [33] result in widths $\Gamma(J/\psi \to \gamma\eta_c(1S)) \simeq 2.9$ keV, a factor of 2 larger than the data [34].**

- **Quark models fail to reproduce the measured branching width $\Gamma(J/\psi \to \gamma\eta_c)$ and, instead, obtain a significantly larger value [10].**

- **Constituent quark models describe the radiative transitions of J/ψ, $\psi(2S)$, χ_{cJ}, h_c and $\psi(3770)$ [16], but the numerical results differ from the worldwide data.**

- **Lattice QCD [19,20] carried out on the radiative transition properties of χ_{c0}, χ_{c1}, however, good descriptions are still not obtained due to technical restrictions.**

- **Cornwell potential model [30] with a complete factorization of m_c provides numerical results different from the worldwide data.**

[10] M. B. Voloshin, Prog. Part. Nucl. Phys. 61, 455 (2008)
[12] T. Barnes, S. Godfrey, and E. S. Swanson, Phys. Rev. D 72, 054026 (2005)
[16] Wei-Jun Deng et al., Phys. Rev. D95, 034026(2017)
[19] Y. Chen et al., Phys. Rev. D 84, 034503 (2011)
[20] D. Becirevic and F. Sanfilippo, J. High Energy Phys. 01 (2013) 028
[30] R. Bruschini and P. González, Phys. Rev. D 101, 014027 (2020).
[33] P. Guo and T. Yepez-Martínez, and A. P. Szczepaniak, Phys.Rev. D 89, 116005 (2014)
[34] P. A. Zyla et al. (Particle Data Group), Prog. Theor. Exp. Phys. 2020, 083C01 (2020)

CCQM approach

- **Based on QFT framework for treatment of bound states using the Weinberg-Salam (WS) compositeness condition.**

- **Manifestly Lorentz invariant, consistent with symmetries of SM and consistently incorporates symmetry breakings.**

- **All bound systems are considered by using the same theoretical principles. Direct inclusion of many-quark states.**

- **Goes beyond the nonrelativisitc picture without spoiling 'classic' results and taking into account relativistic effects by using QFT approach. The nonrelativistic limit can be straightforwardly considered in our approach.**

- **Wide application to and convincing results obtained in:**

  - ***Strong decays***
  - ***Electroweak transitions***
  - ***Heavy meson and boson physics***
  - ***Beyond the Standard Model …***

CCQM main steps

- We derive a phenomenological Lagrangian (Lorenz/Gauge covariant) and describe the interaction of the bound state and its constituents via interpolating quark currents. The required quantum numbers J^{PC} of the bound state are set up via construction of interpolating currents in terms of field operators of the constituents.

- The coupling constant of the bound state ***H*** with its constituents is fixed by solving the ***WS*** condition for vanishing of the renormalization function of the bound state $Z_H = 0$. The bound state is always dressed.

- We construct the S-matrix operator, which consistently generates matrix elements, represented by a set of Feynman diagrams, which are calculated by using the QFT methods. Loop integration corresponding to a Feynman diagram is performed in Euclidean region by using the Wick rotation.

- The convergence of Feynman diagrams is guaranted by introducing the cutoff regularization consistent with gauge invariance. In Euclidean region all loop integrals are well-defined and finite due to an appropriate use of a cutoff regularization by introducing Gassian exponentials. After performing the loop integration we do the continuation of matrix elements into Minkowski space. We have not singularities like *~exp(x)*.

- Hadrons *H(x)* interact by *quark exchanges,* with hadron-quark coupling g_H.

$$L_{\text{int}} = g_H H(x) J_H(x)$$

- Interpolating quark current (for meson):

$$J_H(x) = \int dx_1 \int dx_2\, F_H(x; x_1, x_2)\, \bar{q}(x_2) \Gamma_H q(x_1) \qquad \Gamma_P = i\gamma^5; \quad \Gamma_V = \gamma^\mu$$

- Vertex function (trans. inv.)

$$F_H(x; x_1, x_2) = \delta(x - \omega_1 x_1 - \omega_2 x_2) \cdot \Phi_H(|x_1 - x_2|^2) \qquad \omega_j = m_j / (m_1 + m_2)$$

$$\Phi_H(-p^2) = \exp\left(\frac{p^2}{\Lambda_H^2}\right)$$

Λ_H ~ **hadron "size"**

- Quark propagator **(**in the Schwinger representation**):**

$$S_m(\hat{p}) = \frac{m + \hat{p}}{m^2 - p^2} = (m + \hat{p}) \cdot \int_0^\infty d\alpha_1 \exp\left[-\alpha_1 \left(m^2 - p^2\right)\right]$$

- The ***compositeness condition*** eliminates the bare fields from consideration.

$$Z_H = \left\langle H_{bare} \,|\, H_{phys} \right\rangle^2 = 1 - g_{ren}^2 \, \Pi_H^{'}(M_H^2) = 0$$

PRD81, 034010 (2010)

- Any hadronic matrix element containing loops can be written in the simplex form

$$\Pi^0 = N_c \int_0^\infty dt\, t^{n-1} \int_0^1 d^n\alpha \; \delta\left(1 - \sum_{i=1}^{n} \alpha_i\right) f(t\alpha_1, t\alpha_2, \ldots, t\alpha_n)$$

- The integral diverges for t → ∞, if the kinematic variables allow for the appearance of branch points corresponding to the creation of free quarks.

$$\Pi^0 = N_c \int_0^{1/\lambda^2} dt\, t^{n-1} \int_0^1 d^n\alpha \; \delta\left(1 - \sum_{i=1}^{n} \alpha_i\right) f(t\alpha_1, t\alpha_2, \ldots, t\alpha_n)$$

- Threshold singularities disappear by introducing *λ – the* infrared cutoff parameter

- **Infrared confinement** is introduced to guarantee the absence of all possible *thresholds* corresponding to quark production.

Renormalized couplings

- The renormalization coupling g_H is defined from the compositeness condition

$$Z_H = 1 - g_H^2 \tilde{\Pi}'_H(M_H^2) = 0\,, \qquad \tilde{\Pi}'_H(p^2) = \frac{d}{dp^2}\,\tilde{\Pi}_H^{(1)}(p^2)$$

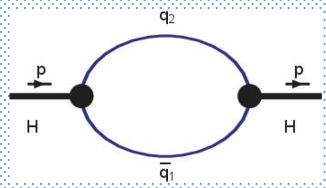

- The requirement $Z_H = 0$ implies that the physical state does not contain the bare state and is appropriately described as a bound state. It effectively excludes the constituent degrees of freedom from the physical state space.

- The interaction leads to a dressed physical particle, i.e. its mass and wave function have to be renormalized.

- For a meson the mass operator corresponding to the self-energy diagram

$$\tilde{\Pi}_H(p) \;=\; N_c \int \frac{dk}{(2\pi)^4 i} \widetilde{\Phi}_H^2\left(-k^2\right) \mathrm{tr}\left[\Gamma_H \widetilde{S}_1(\hat{k} + w_1 \hat{p}) \Gamma_H \widetilde{S}_2(\hat{k} - w_2 \hat{p})\right]$$

Model parameters

A meson in the model is characterized by:

- the global infrared confinement parameter λ (universal)
- the constituent quark masses m_1 & m_2
- the meson size parameter Λ_H (free)

- totally **1+4+N** parameters for **N** hadrons → **1 + 5/N ≈ 1** per hadron

+ The model parameters are determined by minimizing χ^2 in a fit to the latest data and some lattice results. The errors of the fitted parameters are of order ~ 10%

- Global central values of model parameters: (variation ± 10%)

$$\lambda = 0.181\,\text{GeV},$$
$$m_{ud} = 0.241\,\text{GeV}, \quad m_s = 0.428\,\text{GeV},$$
$$m_c = 1.67\,\text{GeV}, \quad m_b = 5.07\,\text{GeV}$$

- Central values of the **size parameters** Λ_H (in GeV)

π	K	D	D_s	B	B_s	B_c	η_c	η_b	
0.87	1.02	1.71	1.81	1.90	1.94	2.50	2.06	2.95	
ρ	ω	Φ	J/ψ	K*	D*	D^*_s	B*	B^*_s	ϒ
0.61	0.50	0.91	1.93	0.75	1.51	1.71	1.76	1.71	2.96

Matrix elements

The invariant matrix element for the one-photon radiative transition $X_1 \to \gamma X_2$

$$\mathfrak{M}_{X_1\to\gamma X_2} = i(2\pi)^4\delta^4(p-q_1-q_2)\,\varepsilon_{X_1}\varepsilon_{X_2}\varepsilon_\gamma\,T_{X_1\to\gamma X_2}(q_1,q_2)$$

In **LO**, transition amplitude $T_{X1\to\gamma X2}(q_1, q_2)$ is described by **'triangle'+ 'bubble' diagrams**

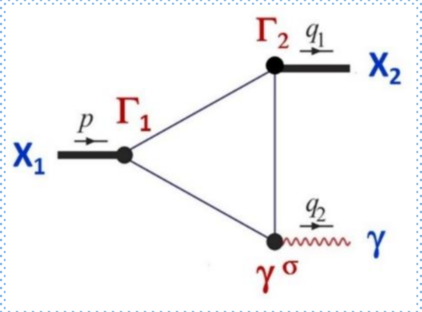

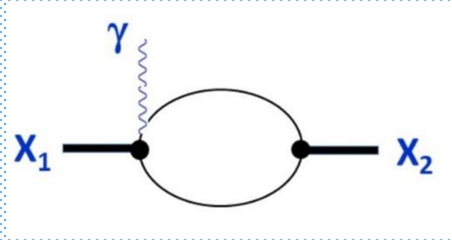

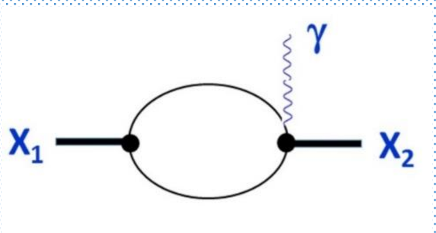

The contributions given by the bubble-type diagrams are small and do not exceed the common errors (±10%) of our calculations.

Taking into account the uncertainty of the experimental data, we drop the bubble-type diagrams without loss in accuracy of our estimates.

Transition amplitude

$$T_{X_1\to\gamma X_2}(q_1,q_2)=g_{X_1}g_{X_2}e_c e N_c\iiint\limits_0^1 d\alpha_1\, d\alpha_2\, d\alpha_3$$

$$\cdot\int\frac{d^4k}{(2\pi)^4 i}\exp\left\{k^2(\alpha_1+\alpha_2+\alpha_3+s_1+s_2)+2k^\nu R^\nu+R_0\right\}$$

$$\cdot\,\mathrm{tr}\left[\Gamma_2(m_c+\hat{k}+\tfrac{1}{2}\hat{p})\,\Gamma_1(m_c+\hat{k}-\tfrac{1}{2}\hat{p})\gamma^\sigma(m_c+\hat{k}-\tfrac{1}{2}\hat{p}+\hat{q}_2)\right]$$

$$=T^{inv}_{X_1,X_2,\gamma}(q_1,q_2)+T^{res}_{X_1,X_2,\gamma}(q_1,q_2).$$

$$q_2^\sigma\cdot T^{(inv)}_{X_1\to\gamma X_2}(q_1,q_2)=0.$$

$$\Gamma_1=\{\gamma^\mu, I, \gamma^\mu\gamma_5,\ \overleftrightarrow{\partial}_\nu\gamma^5, i(\gamma^\mu\overleftrightarrow{\partial}_\nu+\gamma^\nu\overleftrightarrow{\partial}_\mu)/2\}$$

$$T^{(inv)}_{X_1\to\gamma X_2}(q_1,q_2)=\frac{g_{X_1}\,g_{X_2}\,e_c\,e\,N_c}{(2\pi)^2}\int\limits_0^{1/\lambda^2}dt\frac{t^2}{(s+t)^2}\iiint\limits_0^1 d\alpha_1\,d\alpha_2\,d\alpha_3\,\delta(1-\alpha_1-\alpha_2-\alpha_3)$$

$$\cdot f_{\Gamma_1,\Gamma_2}(p,q_1,q_2,m_c,s,t,\alpha_1,\alpha_2,\alpha_3)\cdot\exp\left(-t\,z_0+\frac{t\,s}{s+t}\,z_1+\frac{s^2}{s+t}\,z_2\right),\ (1$$

G.Ganbold, T.Gutsche, M.A.Ivanov, V.Lyubovitskij
Phys.Rev.D 104 (2021) 094048

$$T^{(inv)\rho\sigma}_{J/\psi\to\gamma\eta_c} = g_{J/\psi}\, g_{\eta_c}\, C(p^2, q_1^2, q_2^2)\, \epsilon^{q_1 q_2 \rho\sigma},$$

$$T^{(inv)\rho\sigma}_{\chi_{c0}\to\gamma J/\psi}(q_1, q_2) = g_{\chi_{c0}}\, g_{J/\psi}\, d(p^2, q_1^2, q_2^2)\cdot\left(q_1^\sigma q_2^\rho - g_{\rho\sigma}(q_1\cdot q_2)\right)$$

$$\begin{aligned} T^{(inv)\mu\rho\sigma}_{\chi_{c1}\to\gamma J/\psi}(q_1, q_2) \;&=\; g_{\chi_{c1}}\, g_{J/\psi}\, [\epsilon^{q_2\mu\sigma\rho}(q_1\cdot q_2)\, W_1 + \epsilon^{q_1 q_2\sigma\rho} q_1^\mu\, W_2 \\ &+\; \epsilon^{q_1 q_2 \mu\rho} q_2^\sigma\, W_3 + \epsilon^{q_1 q_2\mu\sigma} q_1^\rho\, W_4 - \epsilon^{q_1\mu\sigma\rho}(q_1\cdot q_2)\, W_4] \end{aligned}$$

$$\begin{aligned} H_L \;&=\; i g_{\chi_{c1}}\, g_{J/\psi}\, \frac{M^2_{\chi_{c1}}}{M_{J/\psi}} |\vec{q}_2|^2 \Big[W_1 + W_3 - \frac{M^2_{J/\psi}}{M_{\chi_{c1}}|\vec{q}_2|} W_4\Big], \qquad |\vec{q}_2| = \frac{M^2_{\chi_{c1}} - M^2_{J/\psi}}{2M_{\chi_{c1}}}, \\ H_T \;&=\; -i g_{\chi_{c1}}\, g_{J/\psi}\, M_{\chi_{c1}} |\vec{q}_2|^2 \Big[W_1 + W_2 - \Big(1 + \frac{M^2_{J/\psi}}{M_{\chi_{c1}}|\vec{q}_2|}\Big) W_4\Big]. \end{aligned}$$

$$T^{(inv)\rho\sigma}_{h_c\to\gamma\eta_c}(q_1, q_2) = g_{h_c}\, g_{\eta_c}\, h(p^2, q_1^2, q_2^2)\cdot\left(q_2^\rho q_1^\sigma - g_{\rho\sigma}(q_1\cdot q_2)\right)$$

$$\begin{aligned} T^{(inv)\mu\nu\rho\sigma}_{\chi_{c2}\to\gamma J/\psi}(q_1, q_2) = g_{\chi_{c2}}\, g_{J/\psi}\, &\Big\{ A\cdot\Big(g^{\mu\rho}\Big[g^{\sigma\nu}(q_1\cdot q_2) - q_1^\sigma\, q_2^\nu\Big] + g^{\nu\rho}\Big[g^{\sigma\mu}(q_1\cdot q_2) - q_1^\sigma\, q_2^\mu\Big]\Big) \\ &+ B\cdot\Big(g^{\sigma\rho}\Big[q_1^\mu\, q_2^\nu + q_1^\nu\, q_2^\mu\Big] - g^{\mu\sigma} q_1^\nu\, q_2^\rho - g^{\nu\sigma} q_1^\mu\, q_2^\rho\Big)\Big\}, \end{aligned} \tag{40}$$

Modified Vertex for Charmonium

CCQM: The non-local vertex function $\Phi_H(-p^2)$ characterizes the quark distribution inside the hadron. It is unique for the given hadron, each hadron has its own adjustable parameter Λ_H related to the hadron 'size'.

$$\Lambda_X = \{\Lambda_{\eta_c}, \Lambda_{J/\psi}, \Lambda_{\chi_{c0}}, \Lambda_{\chi_{c1}}, \Lambda_{h_c}, \Lambda_{\chi_{c2}}\}$$

These charmonium members have the same quark content and possess physical masses in a relative narrow interval $\sim 3 \div 3.5$ GeV.
For this specific case we use the Ansatz: the charmonium 'size' is proportional to its physical mass, i.e., $\Lambda_X = \varrho \cdot M_X$ with $\varrho > 0$ - a common adjustable parameter:

$$\varrho \equiv \Lambda_X / M_X$$

Subsequently, we further use the charmonium *vertex function* defined as

$$\widetilde{\Phi}_X\left(-p^2\right) = \exp\left(\frac{1}{\varrho^2} \cdot \frac{p^2}{M_X^2}\right)$$

Phys.Rev.D 104 (2021) 094048

Numerical results

For further numerical evaluation we keep the basic CCQM parameters:
♦ the universal infrared cutoff parameter $\lambda = 0.181$ GeV
♦ the constituent charm quark mass in the range of ±10% around $m_c = 1.67$ GeV.

♦ We vary $\varrho > 0$ to fit the latest experimental data from PDG-2021.

Renormalization couplings

First we calculate g_H .
They are strictly fixed by the compositeness requirements and do not constitute further free parameters, although keep indirect dependencies on basic model parameters.

Phys.Rev.D 104 (2021) 094048

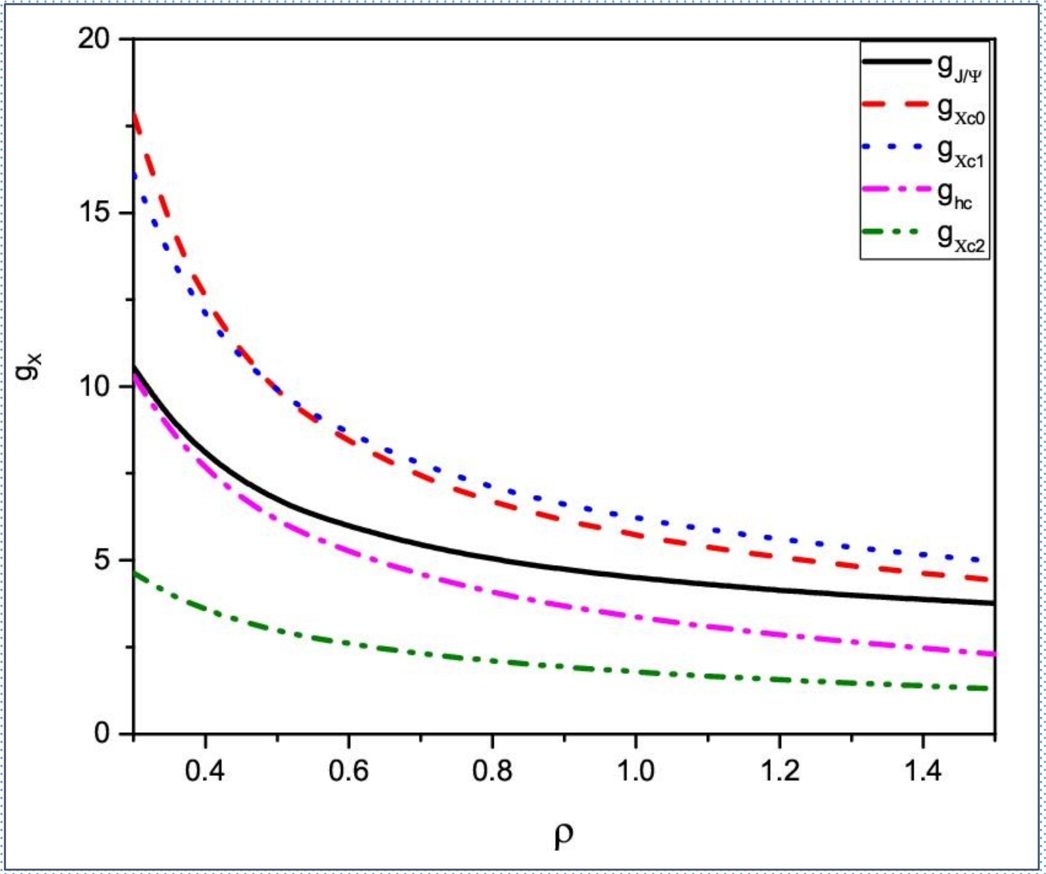

Having calculated g_x we are able to estimate the partial widths of the one-photon radiative decays of the excited (*L=1*) charmonium states χ_{c0} , χ_{c1} and χ_{c2} to find the optimal values of the 'slope' parameter $\varrho > 0$ at different

$m_c \in [1.78 \div 1.82]$ GeV

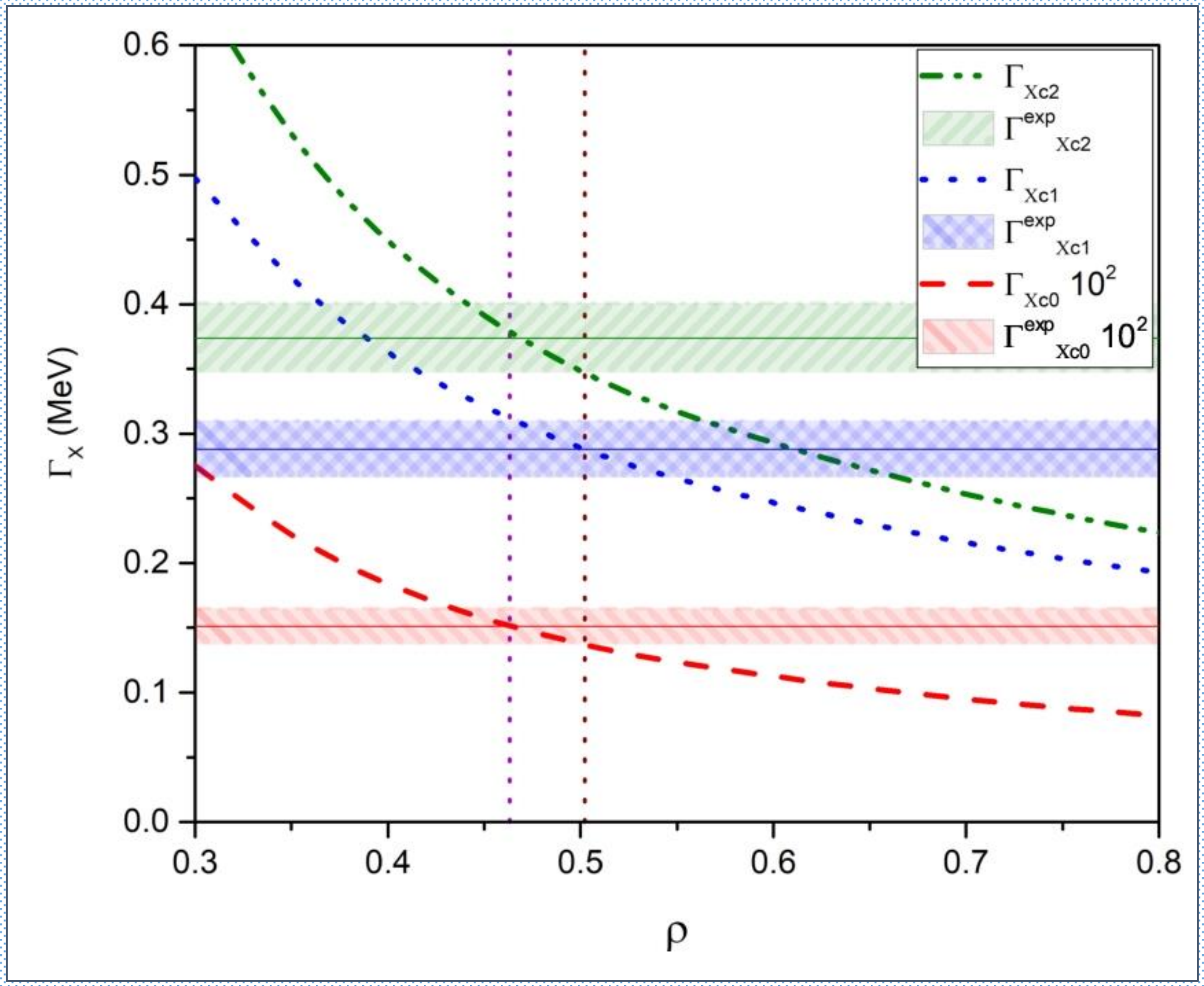

Having calculated g_x we are able to estimate the partial widths of the one-photon radiative decays of the excited (***L=1***) charmonium states χ_{c0} , χ_{c1} and χ_{c2} to find the optimal values of the c-quark mass $\mathbf{m_c}$ at different 'slope' parameter $\varrho > 0$.

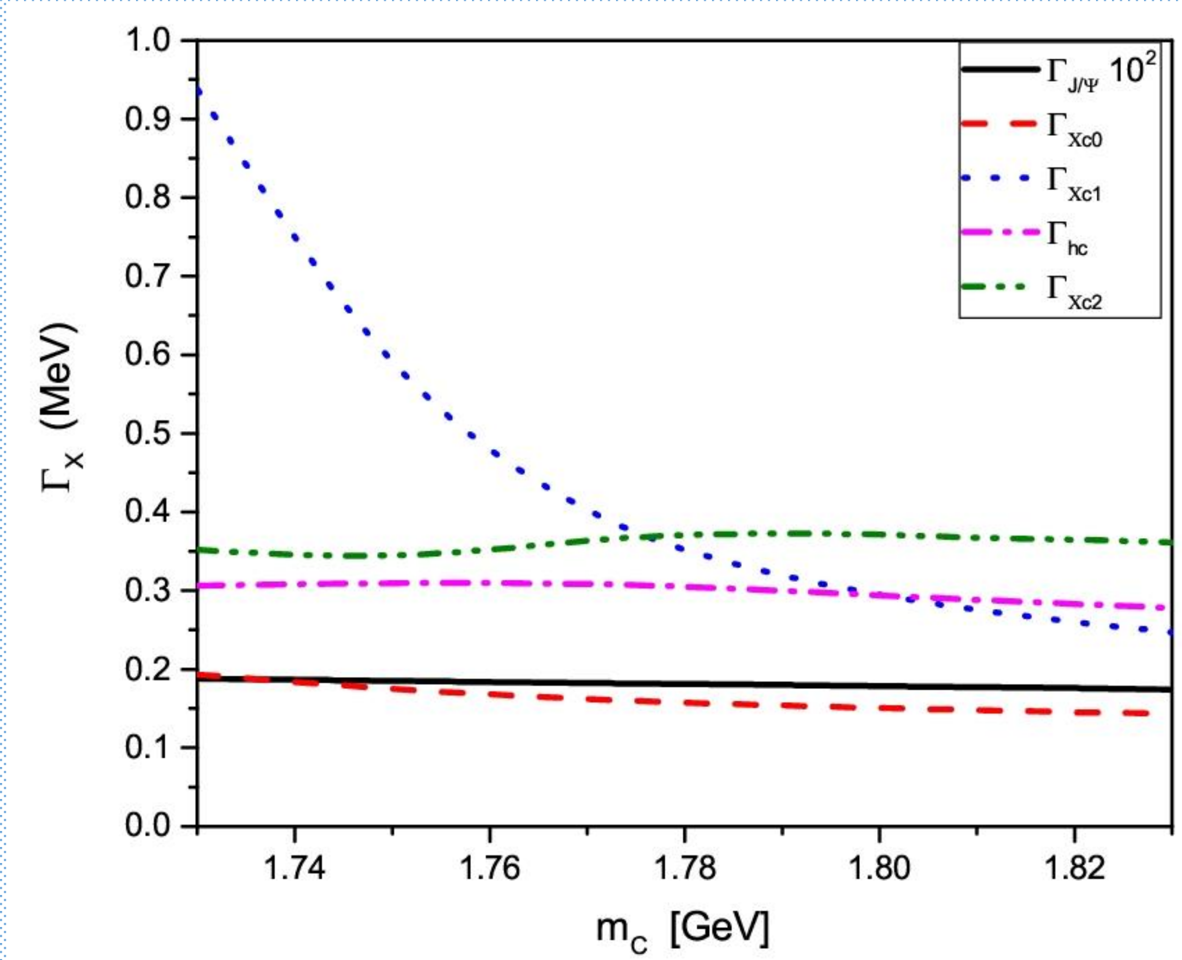

$\varrho \in [0.47 \div 0.53]$

Finally by fitting the latest experimental data PDG-2021 on the partial widths of the dominant one-photon radiative decay of the orbitally-excited charmonium states χ_{c0}, χ_{c1} and χ_{c2} we fix the optimal values of model parameters.

Having fixed the model parameters we calculate the partial widths of the dominant one-photon radiative decays of the ground ($J/\psi \to \gamma + \eta_c$) and orbital-excited ($h_c \to \gamma + J/\psi$) states in dependence on ϱ, together with the curves for χ_{cJ}, J={0,1,2}

λ = 0.181 MeV

m_c = 1.80 GeV

ϱ = 0.485

Phys.Rev.D 104 (2021) 094048

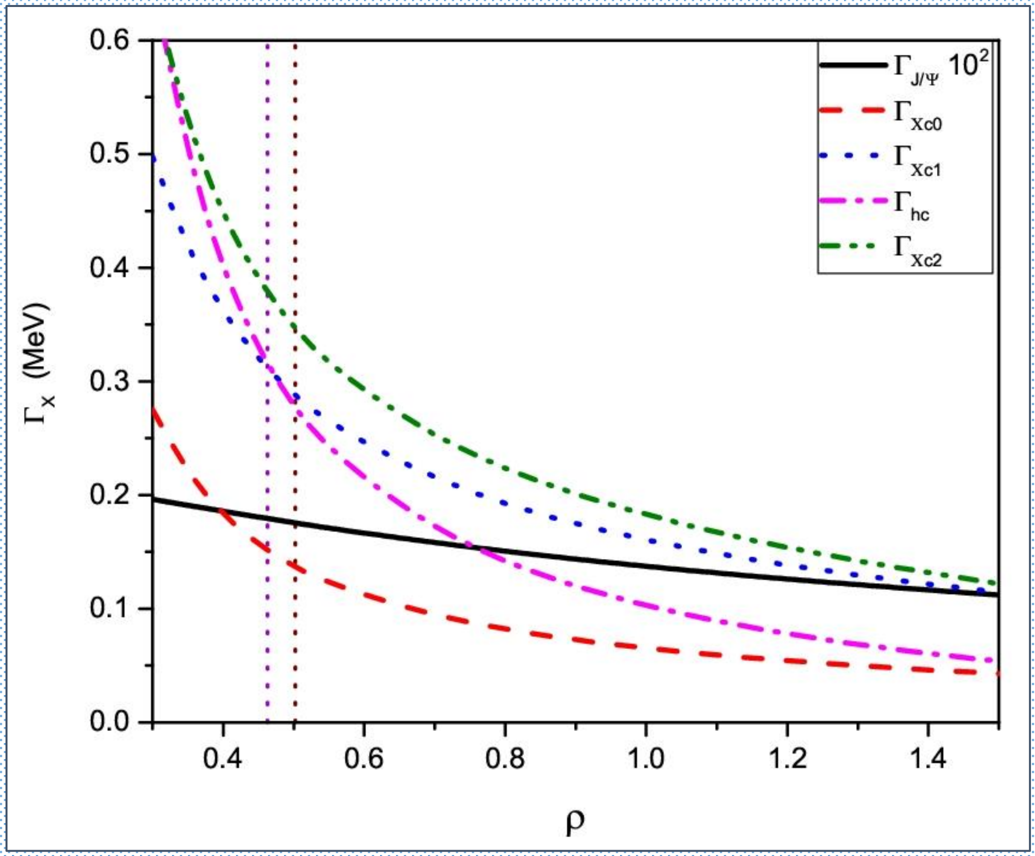

Some theoretical predictions of the partial widths (in units of keV) of the dominant radiative decay of the charmonium states below the $D\bar{D}$ threshold in comparison with recent data.

J^{PC}	Radiative Decay	CCQM λ=0.181	CCQM λ=0	PDG-2021	Cornwell potential [30]	Cornwell potential LWL[30]	Lattice QCD [20]	Constit.Q.M [16]
1^{--}	$\Gamma(J/\psi \to \gamma + \eta_c)$	1.771	1.771	1.58 ± 0.43			2.64(11)	1.25
0^{++}	$\Gamma(\chi_{c0} \to \gamma + J/\psi)$	142.0	142.0	151 ± 14	118	128		128
1^{++}	$\Gamma(\chi_{c1} \to \gamma + J/\psi)$	296.7	297.0	288 ± 22	315	266		275
1^{+-}	$\Gamma(h_c \to \gamma + \eta_c)$	290.8	290.7	357 ± 270			720(50)(20)	587
2^{++}	$\Gamma(\chi_{c2} \to \gamma + J/\psi)$	358.1	356.7	374 ± 27	419	353		467

Phys.Rev.D 104 (2021) 094048

+ $\Gamma(\chi_{cJ} \to \gamma + J/\psi)$ results are close to the recent LHCb data.

+ $\Gamma(J/\psi \to \gamma + \eta_c)$ = 1.77 keV slightly (~12 %) exceeds the recent average data.

+ $\Gamma(h_c \to \gamma + \eta_c)$ = 0.291 MeV leads to *'theoretical full decay width'* $\Gamma^{theor}(h_c) \simeq (0.57 \pm 0.12)$ MeV.

Deconfinement limit

The infrared cutoff parameter in CCQM plays an important role by removing all possible threshold singularities corresponding to the creation of free quarks, and is taken to be universal ($\lambda = 0.181$ GeV) for all physical processes.
However, in some specific cases these singularities do not appear.
Particularly, for $m_c = 1.80$ GeV we obtain $M_X < 2m_c$ for all charmonium states under consideration and the corresponding integrals converge.
Then, we can use even the full integration range $t \in [0, \infty)$, i.e., with $\lambda \to 0$.

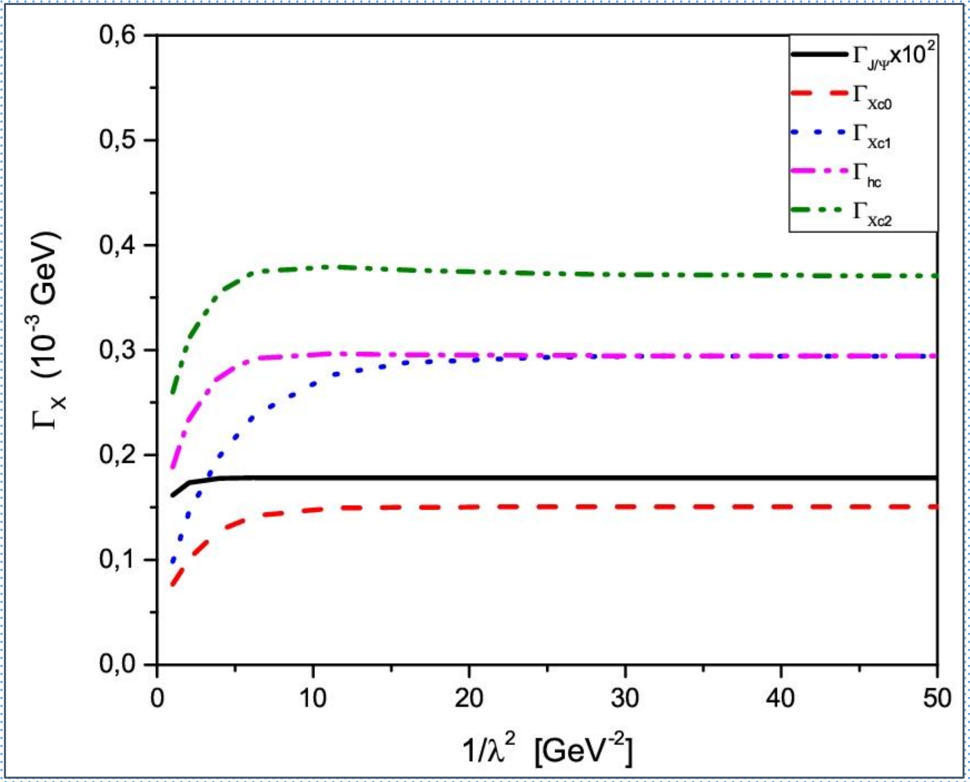

The partial decay widths do not change for $1/\lambda^2 > 20$ GeV^{-2} while $\lambda = 0.181$ GeV corresponds to $1/\lambda^2 = 30.52$ GeV^{-2}.

Our theoretical estimates on the charmonium states remain unchanged in the deconfinement limit $\lambda \to 0$.

Phys.Rev.D 104 (2021) 094048

Discussion (short)

♦ Our calculation within the CCQM

$\Gamma(J/\psi \to \gamma+\eta_c) = 1.77$ keV

slightly (about 12%) exceeds the average value of the recent data [PDG-2021].

♦ Our calculations for the central values of the partial decay widths

$\Gamma(\chi_{c0} \to \gamma+J/\psi) = 142.0$ keV ,

$\Gamma(\chi_{c1} \to \gamma+J/\psi) = 296.7$ keV ,

$\Gamma(\chi_{c2} \to \gamma+J/\psi) = 358.1$ keV

are close to the recent LHCb data.

♦ Our calculation within the CCQM

$\Gamma(h_c \to \gamma+\eta_c) = 0.291$ MeV is in agreement with the recent data.

♦ The present world data for the full decay width of $h_c(^1P_1)(3525)$ cannot be used to test the various predictions due to their large uncertainties. On the other hand, the fractional width for the one-photon radiative decay of $h_c(^1P_1)(3525)$ is detected more accurately. By combining the latest value for the fractional width of [PDG-2021] with our estimate we may calculate the *'theoretical full decay width'* for h_c as follows:

$$\Gamma^{theor}(h_c) \simeq (0.57 \pm 0.12)\ \text{MeV}. \qquad (*)$$

Hereby, we admitted a relevant $\sim 10\%$ uncertainty for $\Gamma(h_c \to \gamma+\eta_c)$.
Compared with data $\Gamma^{exp}(h_c) \simeq (0.7\pm0.4)$ MeV [PDG-2021], the 'prediction' (*) is located in a more narrow interval.

Summary and Outlook

- The dominant radiative transitions of the charmonium states $\eta_c(^1S_0)$, $J/\psi(^3S_1)$, $\chi_{c0}(^3P_0)$, $\chi_{c1}(^3P_1)$, $h_c(^1P_1)$ and $\chi_{c2}(^3P_2)$ have been studied within the CCQM.

- The renormalization couplings *strictly exclude* the constituent degrees of freedom.

- We keep the basic parameters $m_c = 1.80$ GeV, $\lambda = 0.181$ GeV and use ***one*** common adjustable parameter ($\varrho = 0.485$ is fixed by fitting the data for the triplet $\chi_{cJ}(^3P_J)$).

- The fractional widths for $J/\psi(^3S_1)$ and $h_c(^1P_1)$ are *in good agreement* with the data.

- By using the fraction data we recalculate the 'theoretical full width' $\Gamma^{theor}(h_c) \simeq (0.57 \pm 0.12)$ MeV compared with latest data $\Gamma^{exp}(h_c) \simeq (0.7 \pm 0.4)$ MeV.

- By gradually decreasing the global cutoff λ we revealed that the *results do not change for any* $\lambda < 0.181$ GeV up to the 'deconfinement' limit $\lambda \to \mathbf{0}$.

- This approach *may be extended* to other sections of hadron physics:
    - light mesons (scalar, isoscalar, …)
    - radial excitations (charmoniums and bottomoniums)
    - heavy meson and baryon decays
    - exotics (tetraquark, X-Y-Z mesonlike objects, …)